Mirroring the image of the Milky Way bar

Author: Josep Morancho i Poyatos, josep.morancho@outlook.com
Facultat de Física, Universitat de Barcelona, Diagonal 645, 08028 Barcelona, Spain.

Advisor: Marcin Bartosz Semczuk, msemczuk@ub.edu

Abstract: The bar pattern speed ($\Omega_{\rm p}$) is a crucial parameter for understanding dynamics of spiral galaxies, which includes our own Milky Way. Measuring the pattern speed of the Milky Way bar is made difficult by observational limitations, such as dust obscuration in the Galactic plane and incomplete coverage of the far side of the bar. This study investigates whether mirroring the near side of the bar and measuring the pattern speed can yield reliable $\Omega_{\rm p}$ estimates using N-body simulations of a barred galaxy. Mock observational samples are generated, incorporating distance uncertainties and cutting out the zone of avoidance.

Our results show that mirroring produces reasonable $\Omega_{\rm p}$ estimates when distance errors are low but suffers from biases at higher uncertainties. The size of the bar region used for measurements also affects accuracy, improving with bar evolution. While promising, the method requires refinement, such as fixing bar region boundaries and implementing realistic selection functions, to ensure robust application to real Milky Way data. Further tests on diverse simulations are recommended.

Keywords: Astrophysics; Galactic morphology; Milky Way; Computational astrophysics; Data analysis; Numerical methods.

SDGs: Industry, innovation, and infrastructure; Quality education; Partnerships for the goals.

I. Introduction

Bars in spiral galaxies are central, elongated overdensities. Approximately two-thirds of all spiral galaxies in the Local Universe host such a central bar (e.g., [4]). Our Galaxy, the Milky Way, also hosts a central bar.

The main properties of bars are their length, strength, and angular rotation frequency, known as the pattern speed $\Omega_{\rm p}$. These properties can affect the dynamics and evolution of galaxies. The pattern speed, for example, can determine the motions of stars through bar orbital resonances.

This is also the case for the Milky Way bar, where accurately determining the value of the bar pattern speed would help in understanding the motions of stars in the Solar Neighbourhood.

Over the years, various studies have estimated the pattern speed of the Milky Way bar using different techniques. Older measurements suggested a fast and short bar with a pattern speed of 50–60 km s^{-1} kpc^{-1} (e.g., [5]; [2]). More recent measurements place the bar pattern speed in the range 33–40 km s^{-1} kpc^{-1} (e.g., [11]; [9]). For a recent review of the Milky Way bar pattern speed, see section 4.8 of [8].

Among the recent measurements, Zhang et al. (2024) [12] presented an interesting approach by utilising a method recently published by Dehnen, Semczuk & Shoenrich (2023) [3] tailored for simulated bars. Zhang et al. (2024) [12] applied this method to a sample of $\sim$ 2k low-amplitude long-period variable (LA-LPV) candidates from Gaia DR3 and obtained a value of $\Omega_{\rm p} = 34.1 \pm 0.6$ km s^{-1} kpc^{-1}.

The LA-LPV sample, although small, covered the entire bar region, and their measurement was further validated using simulations designed to replicate their observational sample.

The small sample of LA-LPV stars analysed by Zhang et al. (2024) [12] is particularly unique, as most general stellar samples from surveys like Gaia are currently limited to mapping only the near side of the Milky Way bar. This limitation is illustrated, for example, in Fig.19 of [1] and more recently in Fig.16 of [6].

The aim of this project is to investigate whether mirroring the near side of the Milky Way bar (in samples such as those in [6]) and applying the Dehnen et al. (2023) [3] method can yield reasonable results. This approach is tested here using an N-body simulation of a barred galaxy.

This paper is organized as follows: Section 2 details the methods used for measuring the bar pattern speed, generating the simulated data, recreating the observational sample, and mirroring the data; Section 3 presents the results obtained; and Section 4 summarizes and discusses the findings.

II. Methods

To achieve the aims of this project, we employ the following techniques, which are described in more detail below.

A. Bar pattern speed measurement

The primary technique employed in this study is the recently published method by Dehnen et al. (2023) [3] for estimating the bar's pattern speed from a single simulation snapshot, based on the continuity equation.

In this method, the bar region [R_0, R_1] is identified as a

continuous range of radial bins, where R_0 and R_1 denote the inner and outer radii of the bar region, respectively.

The bar orientation, ψ, and pattern speed, Ω_p, are determined using the m=2 Fourier method, applied to all star and gas particles within the bar region with a smooth window function.

This approach ensures a consistent measurement of Ω_p, such that ψ and Ω_p derived from the particles satisfy the relationship $\psi = \int \Omega_p dt$.

The Python code implementing this method is publicly available at `https://github.com/WalterDehnen/patternSpeed`.

B. Simulations

The underlying simulation data used to test the mirroring approach is derived from a growing disc simulation suite, previously used by Semczuk et al. (2022) [10] and Dehnen et al. (2023) [3].

Growing disc simulations provide a method for modeling star formation in isolated discs without requiring computationally expensive gas hydrodynamics. In this method, stars are formed with an initial circular velocity coming from the rotation curve and an additional velocity dispersion which is parametrised. The newly formed stars are distributed according to an exponential disc profile, which scalelength grows with time, emulating the inside-out growth.

The star formation rate decreases with time due to the implemented exponential decay and suppression when the bar is formed. Bar formation is inferred from the on-the-fly m=2 Fourier analysis. Star formation is then halted in the region $0.05 < R_{CR} < 0.7$, where R_{CR} is the corotation radius. This mimics gas depletion and the subsequent suppression of star formation within the bar.

In this project, we use data from the fiducial model presented in Dehnen et al. (2023) [3], where the simulation parameters are described in detail. The model is generally designed to loosely mimic the Milky Way and, by the end of the simulation, consists of a barred disc with a mass of $1.2 \times 10^4 M_\odot$ embedded in dark matter halo with a mass of $2.7 \times 10^5 M_\odot$.

The dark matter halo contains 4.2×10^6 particles, while the model includes 2.4×10^6 star particles at 8 Gyr.

C. Mock observational sample

To recreate the observational sample, we incorporate two observational effects that may affect the measurement of the bar pattern speed: dust obscuration in the galactic plane and distance errors.

As a first step, the data must be centered. Next, the simulation data is transformed into heliocentric galactic coordinates (s, ℓ, b, v_r, v_l, v_b). For this transformation, we assume a distance of 8.2 kpc from the galactic center to the Sun and a bar angle of 30 degrees.

1. Dust obscuration

To mimic dust obscuration, stars within the zone of avoidance are excluded. That is, those that satisfy $|b| < \Delta b/2$.

2. Distance errors

To account for distance errors, an uncertainty is added to the distances based on a normal distribution with a relative error σ_s/s. This approach reflects the increasing difficulty of measuring stellar distances as their distance increases.

Since the velocities v_l and v_b are distance-dependent, errors in the distance must be propagated to calculate new velocities. Using the raw distances, the velocities are first transformed into proper motions in the directions of l and b. Then, smeared distances, accounting for the distance errors, are used to recalculate the corresponding smeared velocities.

Both Δb and σ_s/s are parameters to explore.

D. Data mirroring

To mirror the data, the far half of the galaxy is removed, and the near half is reflected across the center.

Before mirroring the data, the disc can be rotated around the z-axis to align the bar with the x-axis. However, due to the symmetry of the bar, this rotation yields the same value when measuring the bar pattern speed.

III. Results

A. Distance smearing

Figure 1 illustrates the impact of the implemented distance smearing and mirroring on bar morphology and kinematics.

A comparison between the left and middle columns shows that distance errors reduce the bar angle. This effect is evident in both the density distribution and the radial velocity map (v_R), which exhibits the characteristic quadrupole signal associated with bars. Additional plots with larger distance errors were generated, revealing an even lower bar angle. These findings align with the conclusions of [7] and [12].

The addition of mirroring, as shown in the right panel, reveals that this process primarily affects the spiral arms. Despite being influenced by distance uncertainties, the symmetry of the bar between smearing and smearing and mirroring remains mostly preserved.

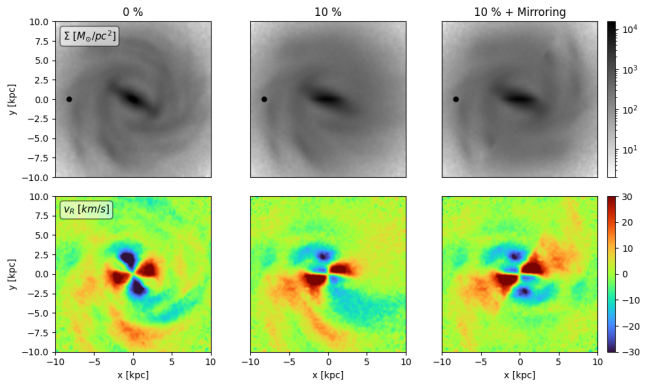

FIG. 1. Stellar density (top) and radial velocity V_R (bottom) at t = 5 Gyr. The left panels show data without uncertainty, the middle panels include 10% distance uncertainty, and the right panels incorporate 10% distance uncertainty and mirroring. The Sun is located at (-8.2, 0) kpc.

B. Bar pattern speed measurements

Figure 3 illustrates how the effects described and implemented in Section II C influence the measurements of the pattern speed in the simulated galaxy. Each grid consists of two rows: the first shows the time evolution of the pattern speed measurements, while the second presents histograms of their relative error.

In the top grid, we observe that the zone of avoidance introduces a small positive bias, which remains below 10% for the largest value of Δb. Thus, cutting out a stripe in galactic latitude and subsequently mirroring the data yields reasonable values for the measurement of Ω_p.

In the middle grid, where distance uncertainties are considered, we observe that the method performs well with a 5% relative distance error. For a 10% relative error, the method initially fails but improves at later times. However, with a 15% relative error, the measurements deviate significantly, showing a large discrepancy between the estimated and true values.

In the bottom grid, when both effects are combined, the method appears to perform better. However, this improvement is merely a numerical coincidence, as the positive bias from the zone of avoidance offsets the negative bias from the distance uncertainty.

C. Effect of the bar region

The accuracy of the bar pattern speed measurement improves over time when a 10% distance uncertainty is applied. This indicates that the method's effectiveness may be influenced by the bar's evolution. To examine this, we assess how well the Dehnen et al. (2023) [3] method estimates other bar parameters in the studied cases and compare these results to the bar's evolution.

Figure 4 shows the time evolution of the inner and outer bar regions, based on both the raw simulation data and the data processed with distance smearing and mirroring, while Figure 2 presents snapshots of the bar region at 5 Gyr and 11 Gyr.

We find that the inner bar radius is consistently overestimated, while the outer radius is underestimated, influenced by the relative distance errors. Both misestimations result in a reduction of the bar region used for pattern speed estimation. However, as the bar grows to roughly twice in size, the bar region used in the method increases over time. This could explain why the estimates become closer to the true values at later times.

Future experiments that fix a specific bar length could further validate this explanation and offer a potential strategy for application to real Milky Way data.

IV. Conclusions

In this project, we wanted to evaluate whether mirroring the near side of the Milky Way bar and applying the Dehnen et al. (2023) [3] method could yield accurate measurements of the bar's pattern speed, despite observational limitations such as dust obscuration and distance uncertainties. We find that this approach gives reasonable results when the relative distance error remains below 10% and the bar's symmetry is preserved through mirroring. However, larger distance uncertainties result in significant deviations in the estimated pattern speed.

Further work is required to fully evaluate the effectiveness of this approach. The simple application of the Dehnen et al. (2023) [3] method to derive both the bar region and the pattern speed can result in underestimating the bar region in some cases and yielding incorrect pattern speed values, with errors of up to 75%.

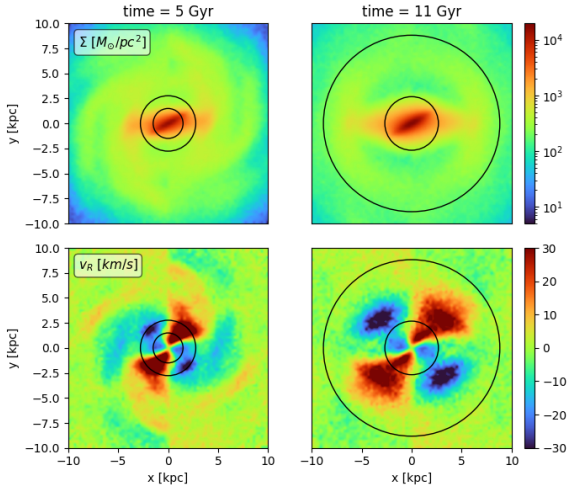

FIG. 2. Surface density (top) and mean radial velocity (bottom) at t = 5 Gyr (left) and t = 11 Gyr (right). The bar region is indicated by circles.

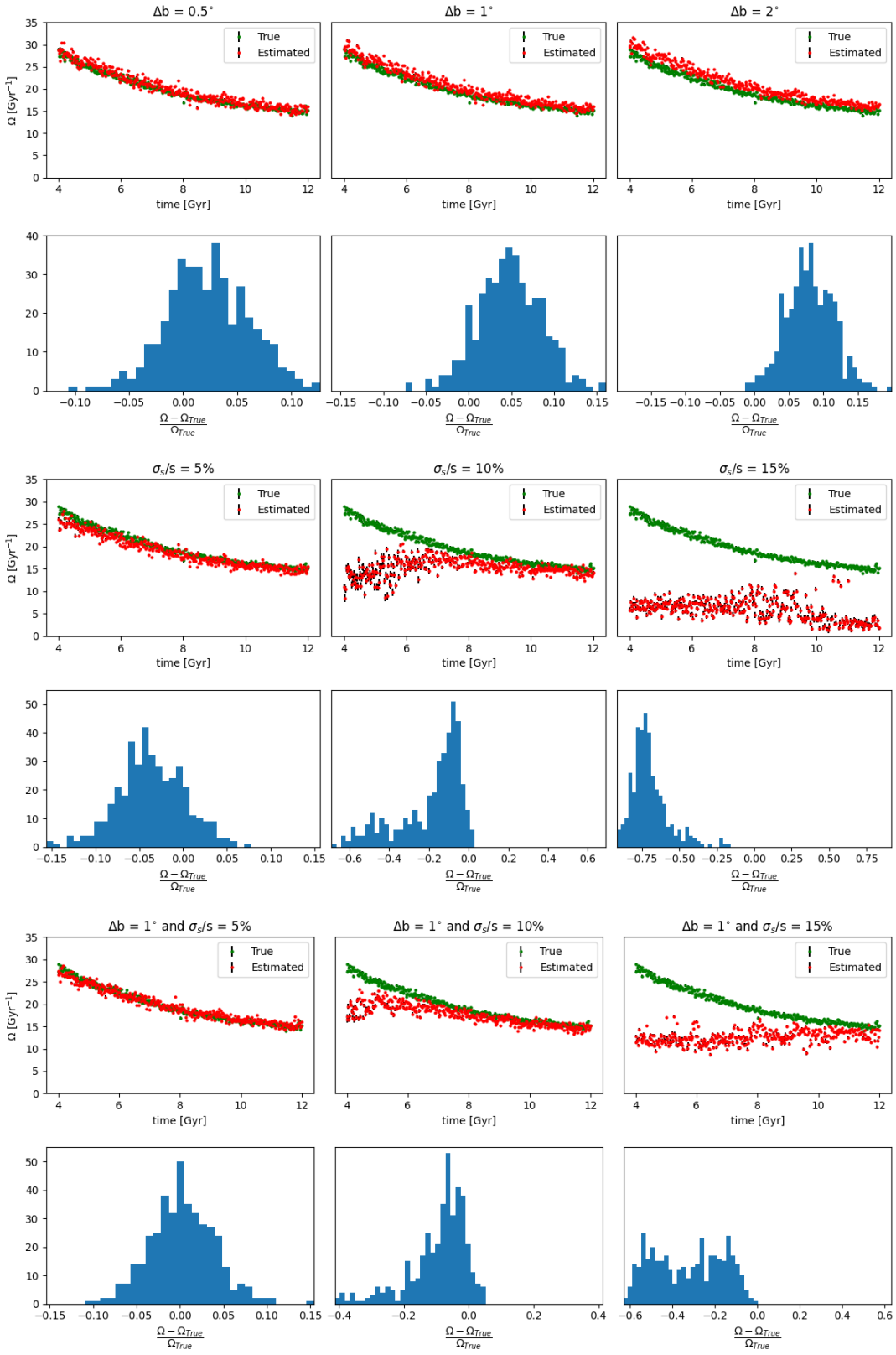

FIG. 3. Time evolution of pattern speed measurements. The top grid shows a zone of avoidance cutout, the middle grid includes distance uncertainty, and the bottom grid combines both. In each grid, the top rows show pattern speed evolution (red: with uncertainty; green: without), and the bottom rows display histograms of relative error.

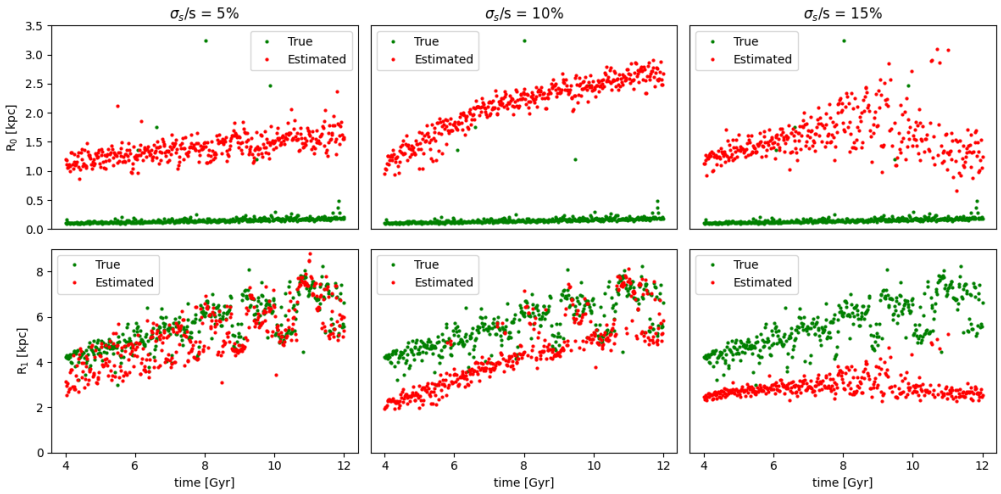

FIG. 4. Time evolution of the inner radius R_0 (top) and outer radius R_1 (bottom) measured from all particles. Panels correspond to distance uncertainties of 5% (left), 10% (middle), and 15% (right). Values without uncertainty are shown in green for comparison.

To address the pattern speed measurement issue caused by distance uncertainty, the inner and outer radii could be fixed at specific values for the measurement. Results of Zhang et al. (2024) [12], where tests were conducted exclusively on smeared data without mirroring, suggest that this approach may be effective.

If this approach proves successful, additional steps could be implemented in the future to enhance the realism of the data. For instance, a more sophisticated selection function could replace the simple straight cut in latitude for the zone of avoidance. Additionally, distance smearing could incorporate errors from Gaia, rather than relying on a normal distribution.

Moreover, as the efficiency of the method within this simulation varied depending on the bar size, conducting additional simulations with a range of bar sizes and shapes will provide a more robust and reliable confirmation.

Acknowledgments

I would like to thank my tutor, Dr. Marcin Bartosz Semczuk, for his invaluable guidance and patience throughout this project. I am also deeply grateful to Marta Puig Subirà, PhD Student at IAA-CSIC and a close friend, for her insightful suggestions on the project and for encouraging me to complete my degree.

[1] F. Anders, A. Khalatyan, C. Chiappini, et al. Photo-astrometric distances, extinctions, and astrophysical parameters for Gaia DR2 stars brighter than G = 18. A&A, 628:A94, Aug. 2019.

[2] V. P. Debattista, O. Gerhard, and M. N. Sevenster. The pattern speed of the OH/IR stars in the Milky Way. MNRAS, 334(2):355–368, Aug. 2002.

[3] W. Dehnen, M. Semczuk, and R. Schönrich. Measuring bar pattern speeds from single simulation snapshots. MNRAS, 518(2):2712–2718, Jan. 2023.

[4] P. Erwin. The dependence of bar frequency on galaxy mass, colour, and gas content - and angular resolution - in the local universe. MNRAS, 474(4):5372–5392, Mar. 2018.

[5] R. Fux. 3D self-consistent N-body barred models of the Milky Way. II. Gas dynamics. A&A, 345:787–812, May 1999.

[6] Gaia Collaboration, R. Drimmel, M. Romero-Gómez, et al. Gaia Data Release 3. Mapping the asymmetric disc of the Milky Way. A&A, 674:A37, June 2023.

[7] D. R. Hey, D. Huber, B. J. Shappee, et al. The Far Side of the Galactic Bar/Bulge Revealed through Semi-regular Variables. AJ, 166(6):249, Dec. 2023.

[8] J. A. S. Hunt and E. Vasiliev. Milky Way dynamics in light of Gaia. *arXiv e-prints*, page arXiv:2501.04075, Jan. 2025.

[9] Z. Li, O. Gerhard, J. Shen, et al. Gas Dynamics in the Milky Way: A Low Pattern Speed Model. ApJ, 824(1):13, June 2016.

[10] M. Semczuk, W. Dehnen, R. Schönrich, and E. Athanassoula. The small boxy/peanut structure of the Milky Way traced by old stars. MNRAS, 509(3):4532–4537, Jan. 2022.

[11] M. C. Sormani, J. Binney, and J. Magorrian. Gas flow in barred potentials - III. Effects of varying the quadrupole. MNRAS, 454(2):1818–1839, Dec. 2015.

[12] H. Zhang, V. Belokurov, N. W. Evans, et al. Kinematics and dynamics of the Galactic bar revealed by Gaia long-period variables. MNRAS, 533(3):3395–3414, Sept. 2024.

Reflectint la imatge de la barra de la Via Làctia

Author: Josep Morancho i Poyatos, josep.morancho@outlook.com
Facultat de Física, Universitat de Barcelona, Diagonal 645, 08028 Barcelona, Spain.

Advisor: Marcin Bartosz Semczuk, msemczuk@ub.edu

Resum: La velocitat angular de la barra ($\Omega_{\rm p}$) és un paràmetre crucial per entendre la dinàmica de les galàxies espirals, entre les quals es troba la Via Làctia. La mesura de la velocitat angular de la barra de la Via Làctia es veu dificultada per limitacions observacionals, com l'obscuriment causat per la pols al pla galàctic i la cobertura incompleta del costat llunyà de la barra. Aquest estudi investiga si reflectir el costat proper de la barra i mesurar la velocitat angular pot proporcionar estimacions fiables de $\Omega_{\rm p}$. Per fer-ho utilitzem simulacions de N-cossos d'una galàxia barrada, a les quals s'incorporen incerteses en les distàncies i s'exclou la zona d'elusió per recrear mostres observacionals.

Els nostres resultats mostren que la reflexió produeix estimacions raonables de $\Omega_{\rm p}$ quan els errors en les distàncies són baixos, però apareixen biaixos quan les incerteses són més altes. La mida de la barra utilitzada en les mesures també afecta la precisió, que millora a mesura que la barra creix. Aquest mètode, tot i que és prometedor, requereix refinaments, com ara fixar els límits de la regió de la barra i implementar funcions de selecció realistes, per assegurar una bona aplicació a dades reals de la Via Làctia. És per això que es recomanen proves addicionals amb diverses simulacions.
Paraules clau: Astrofísica; Morfologia galàctica; Via Làctia; Astrofísica computacional; Anàlisi de dades; Mètodes numèrics.
ODSs: Indústria, innovació, infraestructures; Educació de qualitat; Aliança pels objectius.

Objectius de Desenvolupament Sostenible (ODSs o SDGs)

1. Fi de les desigualtats		10. Reducció de les desigualtats	
2. Fam zero		11. Ciutats i comunitats sostenibles	
3. Salut i benestar		12. Consum i producció responsables	
4. Educació de qualitat	X	13. Acció climàtica	
5. Igualtat de gènere		14. Vida submarina	
6. Aigua neta i sanejament		15. Vida terrestre	
7. Energia neta i sostenible		16. Pau, justícia i institucions sòlides	
8. Treball digne i creixement econòmic		17. Aliança pels objectius	X
9. Indústria, innovació, infraestructures	X		

El contingut d'aquest TFG, part del grau de Física de la UB, es relaciona amb l'ODS 4, i en particular amb la fita 4.7, ja que promou l'educació i la generació de coneixement científic avançat. També es relaciona amb l'ODS 9, fita 9.5, perquè fomenta la investigació científica i l'aplicació de tecnologies avançades per ampliar el coneixement sobre la Via Làctia, contribuint al progrés científic i tecnològic. Finalment, també es pot relacionar amb l'ODS 17, fita 17.6, perquè la recerca astronòmica requereix de col·laboració científica internacional.